Spatial spread of infectious diseases with conditional vector preferences

Frédéric Hamelin, Frank Hilker, Yves Dumont

Spatial spread of infectious diseases with conditional vector preferences

Frédéric M. Hamelin [1,*], **Frank M. Hilker** [2], **Yves Dumont** [3,4,5]

[1] Institut Agro, Univ Rennes, INRAE, IGEPP, 35000, Rennes, France
[2] Institute of Mathematics and Institute of Environmental Systems Research, Osnabrück University, D-49069 Osnabrück, Germany
[3] CIRAD, UMR AMAP, 97410 St Pierre, Réunion Island, France
[4] AMAP, Univ Montpellier, CIRAD, CNRS, INRAE, IRD, Montpellier, France
[5] Department of Mathematics and Applied Mathematics, University of Pretoria, Pretoria, South Africa
* Corresponding author: `frederic.hamelin@institut-agro.fr`

Abstract We explore the spatial spread of vector-borne infections with conditional vector preferences, meaning that vectors do not visit hosts at random. Vectors may be differentially attracted toward infected and uninfected hosts depending on whether they carry the pathogen or not. The model is expressed as a system of partial differential equations with vector diffusion. We first study the non-spatial model. We show that conditional vector preferences alone (in the absence of any epidemiological feedback on their population dynamics) may result in bistability between the disease-free equilibrium and an endemic equilibrium. A backward bifurcation may allow the disease to persist even though its basic reproductive number is less than one. Bistability can occur only if both infected and uninfected vectors prefer uninfected hosts. Back to the model with diffusion, we show that bistability in the local dynamics may generate travelling waves with either positive or negative spreading speeds, meaning that the disease either invades or retreats into space. In the monostable case, we show that the disease spreading speed depends on the preference of uninfected vectors for infected hosts, but also on the preference of infected vectors for uninfected hosts under some circumstances (when the spreading speed is not linearly determined). We discuss the implications of our results for vector-borne plant diseases, which are the main source of evidence for conditional vector preferences so far.

Keywords: vector bias, bistability, backward bifurcation, travelling wave, spreading speed, front reversal, pushed and pulled waves.

1 Introduction

Vector-borne diseases are a major concern for human, animal and plant health. Since Ross' seminal work (1911), most mathematical models of vector-borne infections consider that vectors visit hosts randomly, independent of their infection status (e.g., Wonham et al., 2004; Martcheva, 2015). Spatially explicit models are no exception in this regard (e.g., Lewis et al., 2006). However, growing evidence shows that many vectors do not visit hosts randomly (e.g., Gandon, 2018).

Vectors may be differentially attracted towards infected and uninfected hosts, independent of whether or not they carry the pathogen (e.g., Lacroix et al., 2005; Mauck et al., 2010; Cornet et al., 2013). This is termed a "vector bias" in the modelling literature (Chamchod and Britton, 2011). Kingsolver (1987) was probably the first to include such a vector bias in a model. He showed that vector preferences can induce bistability, meaning that the dynamics converge either to a disease-free state or to an endemic state depending on the initial conditions. However, bistability only occurred in somewhat special cases in which the vector bias was a function of the fraction of infected hosts in the population. Later studies generally assumed a constant vector bias and did not find bistability (Hosack et al., 2008; Chamchod and Britton, 2011; Wang and Zhao, 2017), except when disease-induced host mortality and immigration were included in the model (Buonomo and Vargas-De-León, 2013).

Spatially explicit models have also been used to explore the consequences of a vector bias in space. Individual-based models were formulated to investigate the effect of spatial heterogeneity on the spread of vector-borne diseases with a vector bias (McElhany et al., 1995; Sisterson, 2008). Chamchod and Britton (2011) were probably the first to incorporate a vector bias into a partial differential equation (PDE) model. They numerically showed that travelling waves occur, and how their speed can be calculated. Later studies then also considered a vector bias in PDE models (e.g., Xu and Zhao, 2012; Bai et al., 2018). In particular, Xu and Zhang (2015) also showed the existence of travelling wave solutions. In these studies (Chamchod and

Britton, 2011; Xu and Zhang, 2015), the models did not exhibit bistability, and the travelling waves had positive speeds, meaning that the disease invades a disease-free spatial domain.

Vector preferences, however, may depend on whether or not vectors carry the pathogen (Ingwell et al., 2012; Blanc and Michalakis, 2016; Gandon, 2018; Eigenbrode et al., 2018; Shoemaker et al., 2019; Carr et al., 2020). These are termed "conditional vector preferences". Roosien et al. (2013) were probably the first to include conditional vector preferences in a model, but they did not fully analyse the model. In particular, whether or not bistability can occur was left implicit. In a more general version of the model (accounting for vector handling times), Gandon (2018) showed that conditional preferences (in particular a preference of uninfected vectors for infected hosts) can lead to bistability, provided vector fecundity depends on host infection status. Similarly, Cunniffe et al. (2021) observed multi-stability in a more complex model accounting for vector population dynamics that depend on the host infection status. However, whether conditional preferences can lead to bistability when the vector population dynamics are independent of the host infection status still remains to be clarified.

Bistability may have important implications regarding the spatial spread of the disease in space. In particular, it is well known (Fife and McLeod, 1977; Lewis and Kareiva, 1993; Lewis and van den Driessche, 1993; Owen and Lewis, 2001; Fagan et al., 2002; Hilker et al., 2005, 2007) that bistability can give rise to negative wave speeds, meaning in our context that the disease retreats. This phenomenon is also termed "front reversal".

In this study, we analyse whether and how conditional vector preferences can give rise to bistability and front reversal in vector-borne diseases. The organisation of the paper is as follows. In Section 2, we present a spatio-temporal (reaction-diffusion) model with conditional vector preferences. In Section 3, we provide an analysis of the temporal (non-spatial) model with some numerical simulations. Then, in Section 4, we go back to the spatio-temporal model (with diffusion), showing existence of travelling wave solutions. Numerical simulations illustrate our findings. Lastly, Section 5 concludes the paper with a discussion.

2 Spatio-temporal model

Let $I(x,t)$ be the infected host density at time t and location $x \in \mathbb{R}$. We adopt a uni-dimensional representation of space for simplicity. The total host density is assumed to be a constant N independent of x. The local density of uninfected hosts at time t is therefore $N - I(x,t)$. Let $V(x,t)$ and $U(x,t)$ be the infected ("viruliferous") and uninfected vector densities, respectively. Let b be the vector "biting" rate. Let p and q be the probabilities of pathogen transmission and acquisition, respectively. Let r be the removal rate of infected hosts. Infected vectors lose the pathogen at rate l (Chapwanya and Dumont, 2018). Let m be the vector mortality rate. For simplicity, we assume that the vector birth rate exactly compensates the mortality rate. In addition, we assume that vectors are born uninfected. There is no vertical transmission in either the vector or the host. Let a be the preference (attraction) of infected vectors for uninfected hosts: $a = 1$ means no preference, $a > 1$ preference and $0 < a < 1$ repulsion. Similarly, let u be the preference of uninfected vectors for infected hosts. As in Chamchod and Britton (2011), only the spatial movement of vectors is considered. Let D be the vector diffusion rate, independent of the vector infection status. The model is:

$$\begin{aligned} I_t &= bpV\frac{a(N-I)}{a(N-I)+I} - rI\,, \\ V_t &= bqU\frac{uI}{uI+(N-I)} - (m+l)V + DV_{xx}\,, \\ U_t &= (m+l)V - bqU\frac{uI}{uI+(N-I)} + DU_{xx}\,, \end{aligned} \tag{1}$$

in which the subscripts denote differentiation with respect to t or x, and in which the dependence of the state variables on t and x has been omitted.

2.1 Model simplification

Let $W = U + V$ be the total vector population density. We have $W_t = DW_{xx}$. Assuming $W(x,0) = K$ (the vector carrying capacity) for all $x \in (-\infty, +\infty)$, $W_t(x,0) = 0$ for all x, meaning that $W = K$ for all $t \geq 0$ and $x \in (-\infty, +\infty)$. Therefore, we can substitute

U with $K-V$ in model (1), which thus simplifies to a two-dimensional system:

$$\begin{aligned} I_t &= bpV\frac{a(N-I)}{a(N-I)+I} - rI\,, \\ V_t &= bq(K-V)\frac{uI}{uI+(N-I)} - (m+l)V + DV_{xx}\,. \end{aligned} \tag{2}$$

2.2 Non-dimensionalisation

We rescale the state variables and parameters by letting

$$\tau = (m+l)t\,, \quad \xi = x\sqrt{\frac{m+l}{D}}\,, \quad i = \frac{I}{N}\,, \quad v = \frac{V}{K}$$

and

$$\beta = \frac{bpK}{(m+l)N}\,, \quad \rho = \frac{r}{m+l}\,, \quad \theta = \frac{bq}{m+l}\,.$$

A dimensionless version of model (2) is the following:

$$\begin{aligned} i_\tau &= \beta v\frac{a(1-i)}{a(1-i)+i} - \rho i\,, \\ v_\tau &= \theta(1-v)\frac{ui}{ui+(1-i)} - v + v_{\xi\xi}\,, \end{aligned} \tag{3}$$

in which the subscripts denote differentiation with respect to τ or ξ. Note that the two state variables are both disease prevalences, i.e. they are fractions of the host and the vector being infected, and take values in the unit interval.

3 Analysis of the non-spatial system

The non-spatial model is:

$$\begin{aligned} i' &= \beta v\frac{a(1-i)}{a(1-i)+i} - \rho i =: f_1(i,v)\,, \\ v' &= \theta(1-v)\frac{ui}{ui+(1-i)} - v =: f_2(i,v)\,. \end{aligned} \tag{4}$$

We will also use the following notations: $y = (i,v)^T$ and $f = (f_1, f_2)^T$.

3.1 Basic reproductive number

System (4) was previously explored in Roosien et al. (2013) and Cunniffe et al. (2021). It is known that the disease-free equilibrium $(i, v) = (0, 0)$ is locally asymptotically stable if and only if

$$\mathcal{R}_0^2 := \frac{b^2 pq}{rm} \frac{K}{N} u = \frac{\beta\theta}{\rho} u < 1 \,.$$

We refer to $\mathcal{R}_0^2$ as the basic reproductive number. Note that $\mathcal{R}_0$ depends on u (the preference of uninfected vectors for infected hosts) but does not depend on a (the preference of infected vectors for uninfected hosts). The results we present next are original. Let u_c be such that $\mathcal{R}_0^2 = 1$, i.e.,

$$u_c = \frac{\rho}{\beta\theta} \,.$$

3.2 The system is cooperative

We have

$$\frac{\partial f_1}{\partial v} \geq 0 \quad \text{and} \quad \frac{\partial f_2}{\partial i} \geq 0 \,,$$

since

$$\frac{\partial}{\partial i}\left(\frac{ui}{ui + (1-i)}\right) = \frac{u}{(1 + i(u-1))^2} > 0 \,.$$

Therefore, system (4) is cooperative, meaning that the dynamics necessarily converge to an equilibrium (convergence to a limit cycle is impossible) (Smith, 2008).

3.3 Endemic equilibrium

Let us solve the system $f_1(i, v) = f_2(i, v) = 0$. An endemic equilibrium (i^*, v^*), with $i^*, v^* > 0$, satisfies:

$$Q(i^*) = A{i^*}^2 + Bi^* + C = 0 \,,$$

in which

$$\begin{aligned} A &= (a-1)(u(1+\theta)-1)\,, \\ B &= \left((2-(1+\theta)u)-\frac{\beta\theta}{\rho}u\right)a-1 = -\Big(((1+\theta)u-1)+(\mathcal{R}_0^2-1)\Big)a-1\,, \\ C &= a\left(\frac{\beta\theta}{\rho}u-1\right) = a\left(\mathcal{R}_0^2-1\right). \end{aligned}$$

Let u^* be such that $A=0$:

$$u^* = \frac{1}{1+\theta}\,. \tag{5}$$

Note that A has no reason to be zero in general ($A=0$ only for $a=1$ or $u=u^*$). The coefficient A can be also expressed as

$$A = (a-1)\left(\frac{u}{u^*}-1\right).$$

First, we notice that

$$Q(1) = -u(1+\theta) < 0\,. \tag{6}$$

Next, we distinguish two cases: $\mathcal{R}_0^2 > 1$ and $\mathcal{R}_0^2 < 1$. (The boundary case $\mathcal{R}_0^2 = 1$ is addressed in Appendix A.1 for the sake of completeness.)

3.4 Case $\mathcal{R}_0^2 > 1$

If $\mathcal{R}_0^2 > 1$, then $Q(0) = C > 0$. Since $Q(1) < 0$ (Eq. 6), there is exactly one root i^* in $[0,1]$, which is the endemic equilibrium. Appendix A.2 shows that

$$i^* = \begin{cases} -\frac{C}{B} & \text{if } a=1 \text{ or } u=u^* \quad \text{(special cases implying } A=0)\,, \\ \frac{1}{2A}(-B-\sqrt{\Delta}) & \text{otherwise,} \end{cases}$$

where $\Delta = B^2 - 4AC$ is the discriminant.

3.5 Case $\mathcal{R}_0^2 < 1$

If $\mathcal{R}_0^2 < 1$, then $C < 0$.

Since $Q(0) = C < 0$, and $Q(1) < 0$ (Eq. 6), either there is no root in between 0 and 1 or there are two roots (unless the discriminant Δ is zero, in which case

there is a single root, of course). The existence of biologically feasible equilibria requires $A < 0$. Since this implies $AC > 0$, an additional necessary condition for the existence of endemic equilibria is that the discriminant Δ is non-negative. The additional conditions are $Q'(0) = B > 0$ and $Q'(1) = 2A + B < 0$.

If these conditions ($\mathcal{R}_0^2 < 1$, $A < 0$, $\Delta \geq 0$, $B > 0$, and $2A+B < 0$) are simultaneously satisfied, there are two positive equilibria with components

$$i_{1,2}^* = \frac{1}{2A}\left(-B \pm \sqrt{\Delta}\right), \tag{7}$$

since $A < 0$ and $B > 0$. We set $E_1 = (i_1^*, v_1^*)$ and $E_2 = (i_2^*, v_2^*)$ and notice that the equilibria are ordered, i.e. $E_1 < E_2$, since $i_1^* < i_2^*$ and $v_1^* = g(i_1^*) < v_2^* = g(i_2^*)$, where $g(i) = \dfrac{\rho}{\beta}\left(1 + \dfrac{i}{a(1-i)}\right) i$ is an increasing function corresponding to $f_1 = 0$ in (4).

3.5.1 Necessary conditions for two equilibria

Here, we will derive two necessary conditions on the vector preferences, namely $a > 1$ and $u < u^* < 1$ (since $u^* = 1/(1+\theta)$, as defined in Eq. (5)), for two positive equilibria to coexist.

First, B can be expressed as

$$B = -\left(1 + \theta + \frac{\theta\beta}{\rho}\right) au + (2a - 1)\,.$$

Therefore, $B > 0$ is equivalent to

$$u < \frac{(2a-1)}{\left(1 + \theta + \frac{\theta\beta}{\rho}\right)a} =: u^+\,.$$

Second, $B + 2A < 0$ can be expressed as

$$\left((\theta+1)(a-2) - \frac{\theta\beta}{\rho}a\right)u + 1 < 0\,. \tag{8}$$

A necessary condition for the inequality (8) to hold is

$$\frac{\theta\beta}{\rho(\theta+1)} > \frac{a-2}{a} =: R_1\,. \tag{9}$$

Assuming inequality (9) holds, $B + 2A < 0$ (inequality 8) is equivalent to

$$u > \frac{1}{\frac{\theta\beta}{\rho}a - (\theta+1)(a-2)} =: u^{-} .$$

So far, we have shown that conditions $B > 0$ and $B + 2A < 0$ are equivalent to $u < u^{+}$ and $u > u^{-}$ (provided inequality 8 holds), respectively. A necessary condition for these conditions to hold is therefore $u^{-} < u^{+}$. The latter inequality can be equivalently expressed as

$$\frac{1}{\frac{\theta\beta}{\rho}a - (\theta+1)(a-2)} < \frac{2a-1}{\left(\left(1+\frac{\beta}{\rho}\right)\theta+1\right)a},$$

which is equivalent to

$$\left(1+\frac{\beta}{\rho}\right)\theta + 1 < \left(2-\frac{1}{a}\right)\left(\frac{\theta\beta}{\rho}a - (\theta+1)(a-2)\right).$$

After rearrangement, the above inequality can be equivalently expressed as

$$(\theta+1)(a-1)^2 < a(a-1)\frac{\theta\beta}{\rho}.$$

A necessary condition for the above inequality to hold is $a > 1$. Assuming $a > 1$, this inequality can be equivalently expressed as

$$\frac{\theta\beta}{\rho(1+\theta)} > \frac{a-1}{a} =: R_2 .$$

Since $R_2 > R_1$, the above inequality guarantees that inequality (9) is satisfied.

We were not able to get more results from this preliminary analysis, but we have shown that $a > 1$ is a necessary condition for two endemic equilibria to coexist.

Assuming $a > 1$, the condition $A < 0$ is equivalent to

$$u < \frac{1}{1+\theta} = u^{*} .$$

Hence, $a > 1$ and $u < u^{*} < 1$ are necessary conditions for two positive equilibria to coexist.

3.5.2 Numerical example of bistability

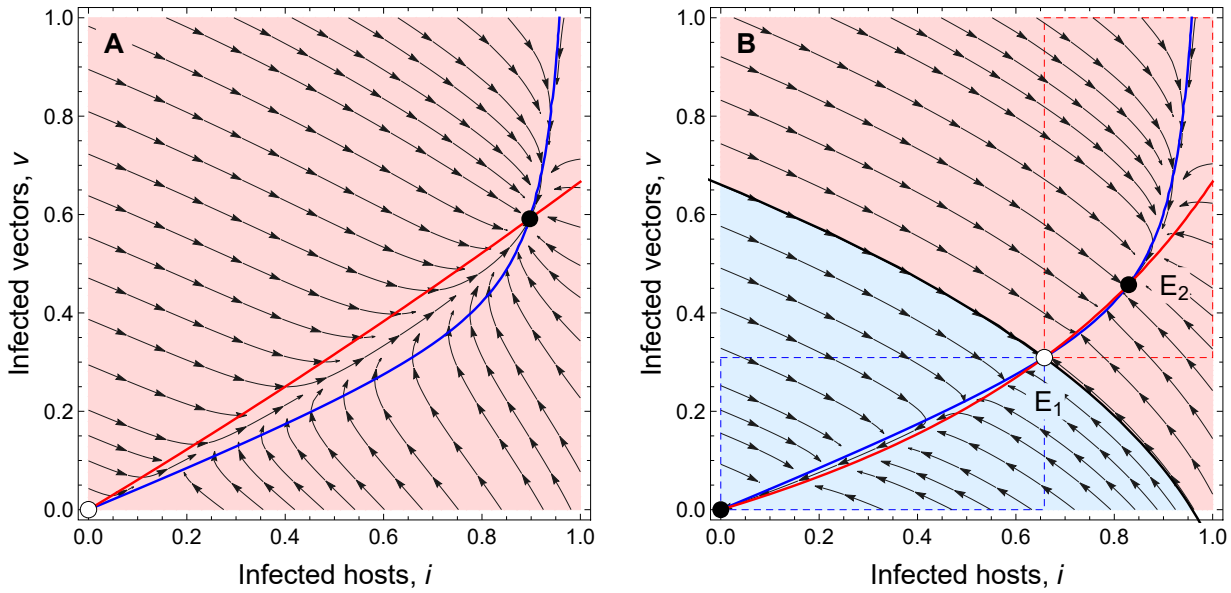

Figure 1: Phase portraits of the non-spatial model (4) with v- and i-nullclines (blue and red curves, respectively). Stable (unstable) equilibria are shown as filled (empty) circles. The basins of attraction to the endemic (disease-free) equilibrium are shown in light red (light blue). (**A**) The endemic equilibrium is the only attractor. Parameter value: $u = 0.3$, so $\mathcal{R}_0^2 = 1.44 > 1$. (**B**) Bistable case. The black line is the separatrix of the two basins of attraction. The dashed rectangles indicate analytically obtained sets of initial conditions that are known to approach the disease-free (blue) or endemic (red) equilibrium. They are part of the actual basins of attraction, see Sect. 3.6 for more details. Parameter value: $u = 0.15$, so $\mathcal{R}_0^2 = 0.72 < 1$. All other parameter values: $a = 15, \beta = 2.4, \rho = 1, \theta = 2$.

Since necessary and sufficient conditions were hardly expressible with pen and paper, we used symbolic calculation software (Maple 2022) to disentangle the conditions for two positive equilibria to coexist. To simplify things, we let

$$X = u(1+\theta) - 1 \quad \text{and} \quad Y = \mathcal{R}_0^2 - 1\,. \tag{10}$$

This way,

$$A = (a-1)X\,, \quad B = -(X+Y)a - 1 \quad \text{and} \quad C = aY\,.$$

Since $\mathcal{R}_0^2 < 1$, $Y < 0$. Since $a > 0$, $C < 0$. The previous section showed that $A < 0$, $a > 1$, and therefore $X < 0$ are necessary conditions for two positive equilibria to coexist. We thus used the function "solve" in Maple to solve the following system of inequalities,

$$A < 0\,, \quad B > 0\,, \quad (2A+B) < 0\,, \quad B^2 - 4AC > 0\,, \quad Y < 0\,, \quad a > 1\,, \quad X < 0$$

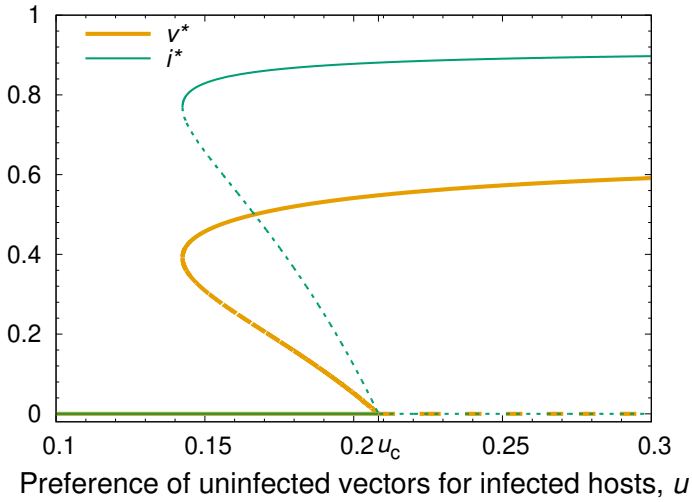

Figure 2: Bifurcation diagram of the non-spatial model (4). Stable (unstable) steady states are shown in solid (dashed) line. There is a backward bifurcation at $u = u_c \approx 0.2083$ and a fold bifurcation at $u \approx 0.1425$. Other parameter values as in Fig. 1.

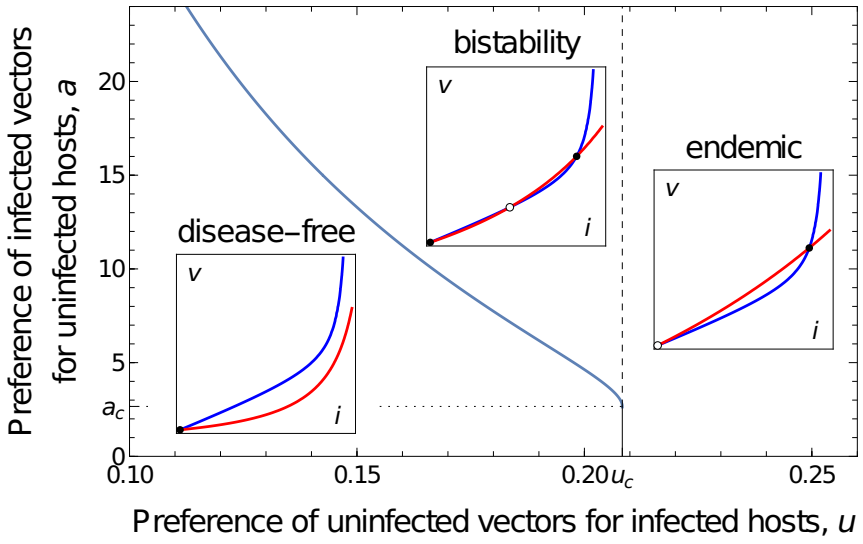

Figure 3: Two-parameter bifurcation diagram of the non-spatial model (4). The fold bifurcation where two endemic equilibria coalesce is shown in blue. The vertical line marks the transcritical bifurcation curve, which occurs at $\mathcal{R}_0^2 = 1$. When the vertical line is solid (dashed), there is a standard transcritical (backward) bifurcation. The fold and transcritical bifurcation curves meet at $(u_c \approx 0.2083, a_c \approx 2.6666)$. The insets are nullcline examples of parameter values leading to different dynamical regimes. Other parameter values as in Fig. 1.

with respect to X ,Y and a. Letting

$$h(Y,a) := \frac{Ya^2-(2Y+1)a-2\sqrt{-Ya^2(a-1)(Y+1)}}{a^2},$$

we obtained the following set of conditions:

- If $1<a<2$,
$$\frac{Ya+1}{a-2} < X < h(Y,a), \quad \text{and} \quad Y > -\frac{a-1}{a}.$$
- If $a=2$,
$$X < -\frac{1}{2} - \sqrt{-Y(Y-1)} = h(Y,2), \quad \text{and} \quad Y > -\frac{1}{2}.$$
- If $a>2$:
$$\begin{cases} X < h(Y,a) & \text{if} \quad Y > -\dfrac{1}{a}, \\ X < -4\dfrac{a-1}{a^2} = h\left(\dfrac{1}{a},a\right) & \text{if} \quad Y = -\dfrac{1}{a}, \\ \text{impossible} & \text{if} \quad Y \in \left[-\dfrac{a-1}{a}, -\dfrac{1}{a}\right), \\ X < \dfrac{Ya+1}{a-2} & \text{if} \quad Y < -\dfrac{a-1}{a}. \end{cases}$$

This condition set allowed us to find parameter values for which bistability occurs; see Figs. 1–3 for phase portraits, one-parameter, and two-parameter bifurcation diagrams, respectively.

3.6 Local and global asymptotic stability

The system being monotone cooperative, proving global asymptotic stability (GAS) relies on local asymptotic stability (LAS) and the use of some appropriate theorems.

The Jacobian of system (4) is

$$J(i,v) = \begin{pmatrix} -\beta v \dfrac{a}{(a(1-i)+i)^2} - \rho & \beta \dfrac{a(1-i)}{a(1-i)+i} \\ \theta(1-v)\dfrac{u}{(ui+(1-i))^2} & -\theta\dfrac{ui}{ui+(1-i)} - 1 \end{pmatrix}.$$

Notice that $J(i,v)$ is irreducible for all $(i,v) \in [0,1)^2$. At equilibrium $(0,0)$, we have

$$J(0,0) = \begin{pmatrix} -\rho & \beta \\ \theta u & -1 \end{pmatrix},$$

from which we deduce that $0 = (0,0)^T$ is LAS when $\mathcal{R}_0^2 = \beta\theta u/\rho < 1$ and unstable when $\mathcal{R}_0^2 > 1$.

When $\mathcal{R}_0^2 > 1$, only one positive endemic equilibrium, E, exists in $[0,1]^2$. Thus, when $\mathcal{R}_0^2 > 1$, using Theorem 6 in Anguelov et al. (2012) (see also Smith, 2008), with $\mathbf{a} = (0,0)$ and $\mathbf{b} = (1,1)$ such that $f(\mathbf{b}) \leq 0 \leq f(\mathbf{a})$, we deduce that the endemic equilibrium E is GAS on $[0,1]^2$. Similarly, when $\mathcal{R}_0^2 < 1$, in the case when no endemic equilibrium exists, we can show, using the same approach, that 0 is GAS.

Assume $\mathcal{R}_0^2 < 1$. In the case where 0, E_1, and E_2 co-exist such that $0 \ll E_1 \ll E_2$, we already know that 0 is LAS. We can check (at least numerically) that E_1 is unstable and E_2 is LAS. Following Smith (2008, Theorem 2.2.2), it is straightforward to show that the set $\{y \in \mathbb{R}^2 : 0 \leq y < E_1\}$ is in the basin of attraction of 0, while the set $\{y \in \mathbb{R}^2 : E_1 < y \leq 1\}$, where $1 = (1,1)^T$, is in the basin of attraction of E_2 (Fig. 1B).

4 Back to the system with diffusion

In this section, we get back to the system with diffusion, i.e., system (3).

4.1 Existence and uniqueness of a solution

System (3), with non-negative initial conditions and appropriate boundary conditions, is a partly dissipative or a partially degenerate system. We consider the following spaces

$$\mathcal{S} = \left\{(i,v) | v \in L^2(\mathbb{R}); i \in L^\infty(\mathbb{R})\right\},$$

and

$$\mathcal{S}_{1,1} = \{(i,v) \in \mathcal{S} | 0 \leq v \leq 1; 0 \leq i \leq 1\}.$$

Following Rothe (1984, Theorem 1, page 111), or Rauch and Smoller (1978, Theorem 2.1), we can show local existence and uniqueness. Then, using a priori L^∞

estimates, the fact that the right-hand side of (3) is quasi-positive and the maximum principle lead to

Theorem 1 (Existence and uniqueness)**.** *For any initial values* $(i_0, v_0) \in \mathcal{S}_{1,1}$*, system (3) admits a unique non-negative bounded solution such that*

$$i \in C([0,\infty); L^\infty(\mathbb{R})) \cap C^1([0,\infty); L^\infty(\mathbb{R}))$$

and

$$v \in C([0,\infty); L^\infty(\mathbb{R})) \cap C\big([0,\infty); H^2(\mathbb{R})\big) \cap C^1\big([0,\infty); L^2(\mathbb{R})\big).$$

Since the study of the non-spatial system showed us that, depending on parameter values, it can be monostable or bistable, it seems relevant to study the existence (or non-existence) of travelling wave solutions.

4.2 Monostable case

In this section, we assume $\mathcal{R}_0^2 > 1$. We know from the non-spatial system that the disease-free equilibrium 0 is unstable and the endemic equilibrium E is GAS. Does a travelling wave solution connecting 0 to E exist?

4.2.1 Existence of a travelling wave

In the monostable case, the existence of a travelling wave should derive from the fact that the system is cooperative (Li et al., 2005); the problem is that the system is partially degenerate (Fang and Zhao, 2009; Li, 2012). However, for this situation powerful theorems exist (Fang and Zhao, 2014; Li, 2012), see also Doli (2017).

Here, we will use Theorem 4.2 in Li (2012) for the following system:

$$\frac{\partial \mathbf{y}}{\partial t} = D\frac{\partial^2 \mathbf{y}}{\partial x^2} + \mathbf{f}(\mathbf{y}(t,x)),$$

with $\mathbf{y} = (y_1(t,x), \ldots, y_k(t,x))$, $D = \mathrm{diag}(d_1, \ldots, d_k) \geq 0$ and $\mathbf{f} = (f_1, \ldots, f_k)$. According to Li (2012), the following hypotheses have to be checked (Hypotheses 2.1 in Li, 2012):

1. There is a proper subset Σ_0 of $\{1, \ldots, k\}$ such that $d_i = 0$ for $i \in \Sigma_0$ and $d_i > 0$ for $i \notin \Sigma_0$.

2. $\mathbf{f}(0) = 0$, there is a constant $\gamma \gg 0$ such that $\mathbf{f}(\gamma) = 0$ which is minimal in the sense that there is no constant ν other than γ such that $\mathbf{f}(\nu) = 0$ and $0 \ll \nu \ll \gamma$, and the equation $\mathbf{f}(\alpha) = 0$ has a finite number of constant roots.

3. The system is cooperative.

4. $\mathbf{f}(\alpha)$ is uniformly Lipschitz in α such that there is $\eta > 0$ such that for any α_i, $i = 1, 2$, $\|(\alpha_1) - \mathbf{f}(\alpha_2)\| \leq \eta \|\alpha_1 - \alpha_2\|$.

5. $\mathbf{f}$ has the Jacobian $\mathbf{f}'(0)$ at 0 with the property that $\mathbf{f}'(0)$ has a positive eigenvalue whose eigenvector has positive components.

Assuming $\mathcal{R}_0^2 > 1$, and $k = 2$, it is straightforward to check the first three hypotheses for system (3), where $\gamma = E$. The fourth hypothesis requires long computations for $a \neq 1$ and $u \neq 1$ to be checked. Lastly, we have

$$\mathbf{f}'(0) = \begin{pmatrix} -\rho & \beta \\ \theta u & -1 \end{pmatrix}.$$

Since $\mathcal{R}_0^2 > 1$, it is straightforward to show that $\mathbf{f}'(0)$ has a positive eigenvalue, $\lambda = \frac{1}{2}\left(\sqrt{(1-\rho)^2 + 4\rho\mathcal{R}_0^2} - (1+\rho)\right)$, associated with the positive eigenvector $\left(1, \frac{\lambda+\rho}{\beta}\right)^T$. Thus, according to Theorem 4.2 in Li (2012), we deduce the existence of a travelling wave connecting 0 to $\gamma = E$. See, for instance, Fig. 4.

4.2.2 Derivation of the linear spreading speed

Still assuming $\mathcal{R}_0^2 > 1$, we consider a travelling front connecting the disease-free equilibrium, 0 to the endemic equilibrium, E. We posit that, in some circumstances, the front speed is linearly determined by the minimum possible wave speed based on the linearisation at the leading edge of the wave. We apply the minimum wave speed approach (Lewis and Schmitz, 1996; Hadeler and Lewis, 2002; Bampfylde and Lewis, 2007; Hilker and Lewis, 2010; Hamelin et al., 2022) to the linearised model to find the linear spreading speed as a critical point. However, we stress that the linear spreading speed may be only a lower bound of the actual spreading speed in some cases (see Fig. 11 in Appendix B.2).

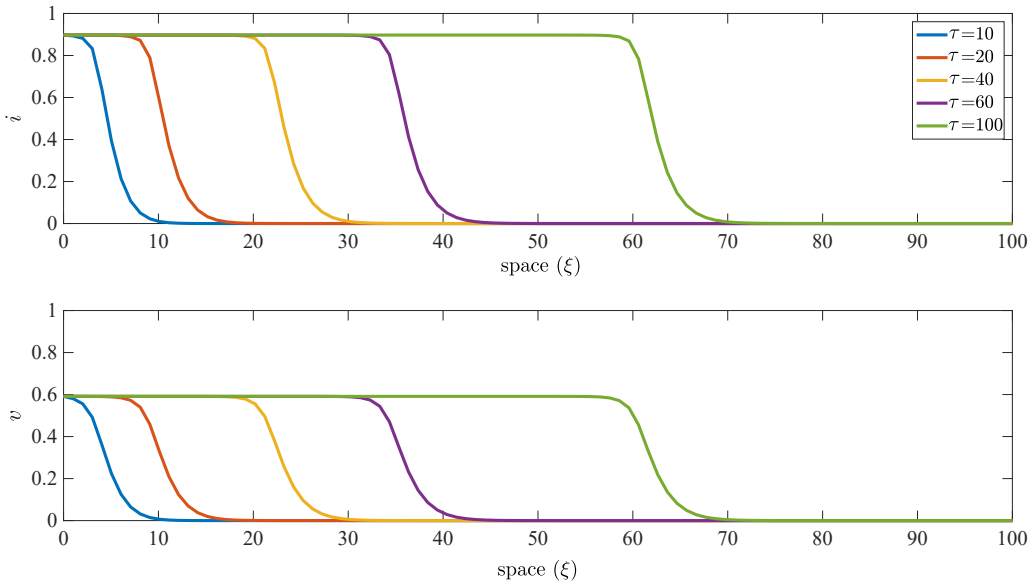

Figure 4: Monostable travelling wave solution of model (3) connecting the disease-free and endemic equilibria 0 and E when $\mathcal{R}_0^2 = 1.44 > 1$. Here $u = 0.3$, other parameter values as in Fig. 1.

At the leading edge of the front invading the disease-free equilibrium, i and v have small positive values. We linearise system (3) at the leading edge:

$$\begin{aligned} i_\tau &= \beta v - \rho i\,, \\ v_\tau &= \theta u i - v + v_{\xi\xi}\,. \end{aligned}$$

We are interested in travelling wave solutions such that

$$y = \begin{pmatrix} i \\ \\ v \end{pmatrix} = k \exp(-s(\xi - c\tau))\,,$$

in which k is an implicit column vector, c is the linear wave speed, and s is the exponential decay rate of the wave profile at leading edge.

Plugging the previous expression in the system, we obtain

$$scy = \underbrace{\begin{bmatrix} -\rho & \beta \\ \\ \theta u & -1 + s^2 \end{bmatrix}}_{M_s} y\,, \tag{11}$$

which implies that

$$\underbrace{\det\begin{bmatrix} -\rho - sc & \beta \\ \theta u & -1 + s^2 - sc \end{bmatrix}}_{M_s - sc\mathbb{I}} = 0\,,$$

in which $\mathbb{I}$ is the identity matrix. This yields

$$\begin{aligned} 0 &= (-\rho - sc)(-1 + s^2 - sc) - \theta u \beta\,, \\ &= Fc^2 + Gc + H\,, \end{aligned} \tag{12}$$

with

$$F = s^2\,, \quad G = s(\rho + 1 - s^2)\,, \quad H = \rho(1 - s^2) - \theta u \beta\,.$$

Next, we follow the approach of using Eq. (12) to calculate the minimum linear wave speed as outlined in Hadeler and Lewis (2002).

The discriminant of the quadratic in Eq. (12) is

$$\begin{aligned} \Lambda &= G^2 - 4FH\,, \\ &= s^2\left((\rho + 1 - s^2)^2 - 4\rho(1 - s^2) + 4\theta u\beta\right)\,, \\ &= s^2\left((\rho - 1 + s^2)^2 + 4\theta u\beta\right) > 0\,. \end{aligned}$$

Since $\Lambda > 0$, there are two real roots:

$$z = \frac{-G - \sqrt{\Lambda}}{2F} \quad \text{and} \quad c = \frac{-G + \sqrt{\Lambda}}{2F}\,.$$

First, we show that $z < 0$. If $G > 0$, then $z < 0$ since $F > 0$. Otherwise (if $G < 0$), then $-G - \sqrt{\Lambda} > 0$ is equivalent to $0 > -4FH$, which is impossible since $H < 0$ (this is because $G < 0$ implies $1 - s^2 < 0$).

Second, we show that $c > 0$ for all $s > 0$. If $G < 0$, then $c > 0$ since $F > 0$. Otherwise (if $G > 0$), then $-G + \sqrt{\Lambda} > 0 \Leftrightarrow \Lambda > G^2$ is equivalent to $\mathcal{R}_0^2 > 1 - s^2$, which is satisfied since we assume $\mathcal{R}_0^2 > 1$ in this section.

The relevant root is therefore c. Since Eq. (12) only depends on three additional

parameters, s, ρ and $\beta\theta u$, we express c as a function of these parameters:

$$c(s,\rho,\beta\theta u) = \frac{-(\rho+1-s^2)+\sqrt{\left(\rho-1+s^2\right)^2+4\theta u\beta}}{2s}\,.$$

Since c is a convex function of s (Appendix B.1), $\lim_{s\to 0} c(s,\rho,\beta\theta u) = +\infty$, and $\lim_{s\to+\infty} c(s,\rho,\beta\theta u) = +\infty$, there exists a minimum to c with respect to $s > 0$.

Equation (12) can also be written to include the dependency of c on s, ρ, and $\beta\theta u$ as

$$P(c(s,\rho,\beta\theta u),s) := (-\rho - sc)(-1+s^2-sc) - \theta u\beta\,.$$

Differentiating with respect to s, we have, for all s,

$$\frac{\mathrm{d}P}{\mathrm{d}s} = \frac{\partial P}{\partial c}\frac{\partial c}{\partial s} + \frac{\partial P}{\partial s} = 0\,. \tag{13}$$

We are interested in the minimum possible linear wave speed. Let

$$s^\star(\rho,\beta\theta u) = \operatorname{arg\,min}_s c(s,\rho,\beta\theta u)\,,$$

and

$$c^\star(\rho,\beta\theta u) = c(s^\star(\rho,\beta\theta u),\rho,\beta\theta u)\,.$$

Since $c^\star$ is such that $\partial c/\partial s = 0$, Eq. (13) yields

$$\frac{\partial P}{\partial s}(c^\star(\rho,\beta\theta u), s^\star(\rho,\beta\theta u)) = 0\,. \tag{14}$$

Since P is cubic in s, $\partial P/\partial s$ is quadratic in s. We are interested in the conditions on the coefficients that allow both polynomials to have a common root, $s^\star$. They are given by cancelling the resultant of the two polynomials. Letting $P = es^3+fs^2+gs+h$ yields $\partial P/\partial s = 3es^2+2fs+g$. The coefficients are identified as

$$e = -c\,,\quad f = c^2-\rho\,,\quad g = (\rho+1)c\,,\quad h = -\theta u\beta+\rho\,.$$

The resultant is $r(e,f,g,h) = -e(f^2g^2-4eg^3-4f^3h+18efgh-27e^2h^2)$, as described in Janson (2010, Eq. (4.3)). The equality $r(e,f,g,h) = 0$ can be equivalently

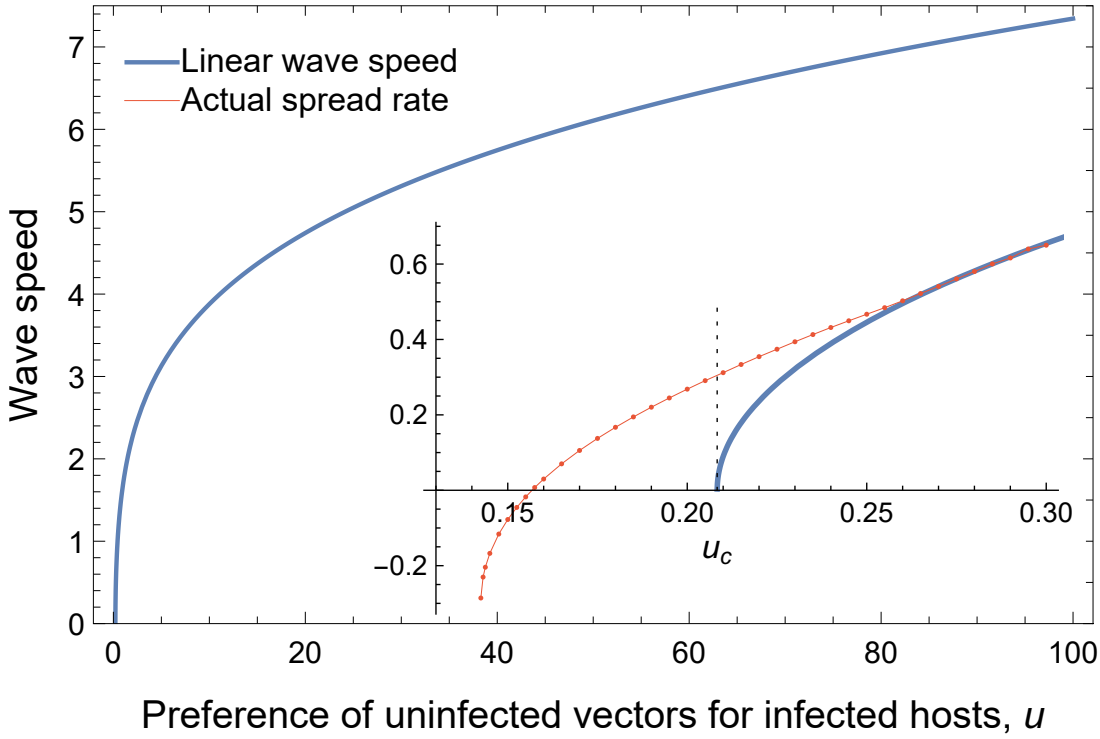

Figure 5: Linear speed of the monostable travelling wave as a function of u (the preference of uninfected vectors for infected hosts). The inset zooms on small values of u and compares the linear and actual (numerically computed) spreading speeds in model (3). The spreading speed is not linearly determined in the bistable case ($u < u_c$) and in the monostable case ($u > u_c$) for u close to u_c. However, the actual speed quickly converges to the linear speed as u increases. Other parameter values as in Fig. 1.

expressed as a cubic with respect to c^2:

$$c_3(c^2)^3 + c_2(c^2)^2 + c_1(c^2)^1 + c_0 = 0\,, \tag{15}$$

with

$$\begin{aligned} c_3 &= 4\beta\theta u + (\rho-1)^2\,, \\ c_2 &= 2\rho^3 + 2\rho^2 + (6\beta\theta u - 8)\rho + 18\theta u\beta + 4\,, \\ c_1 &= \rho^4 + 8\rho^3 - (6\beta\theta u + 8)\rho^2 + 36u\rho\beta\theta - 27u^2\beta^2\theta^2\,, \\ c_0 &= -4\rho^3(\beta\theta u - \rho) = -4\rho^4(\mathcal{R}_0^2 - 1)\,. \end{aligned}$$

Since we assume $R_0^2 > 1$, we have that c_0 is negative and c_3 is positive, which means that we are in the same configuration as Hadeler and Lewis (2002). This implies that $c^\star(\rho, \beta\theta u)$ is uniquely defined as the square root of the largest root of the above cubic.

Although it is possible to write down the formula for the largest root of a cubic polynomial, we have no simple expression of $c^\star(\rho, \beta\theta u)$. Figure 5 shows the minimum linear speed of the monostable travelling wave solution as a function of u, as obtained by solving the cubic equation (15).

4.3 Bistable case

In this section, we assume $\mathcal{R}_0^2 < 1$.

4.3.1 Existence of a travelling wave

To show the existence of a bistable travelling wave solution, we will consider Theorem 4.2 in Fang and Zhao (2009). We have to verify that assumption (L): $f \in C^1(\mathbb{R}^2, \mathbb{R}^2)$ satisfies the following conditions:

1. $f(0) = f(E_2) = f(E_1) = 0$, with $0 \ll E_1 \ll E_2$. There is no η other than 0, E_1 and E_2 such that $f(\eta) = 0$, with $0 \leq \eta \leq E_2$.
2. System (3) is cooperative.
3. $y \equiv 0$ and $y \equiv E_2$ are stable while $y \equiv E_1$ is unstable, that is

$$\lambda_0 := s(f'(0)) < 0, \quad \lambda_{E_2} := s(f'(E_2)) < 0, \quad \lambda_{E_1} = s(f'(E_1)) > 0.$$

4. $f'(0)$, $f'(E_1)$, and $f'(E_2)$ are irreducible.

Assuming that assumption (L) holds, then according to Theorem 4.2 in Fang and Zhao (2009), system (3) admits a monotone wavefront (U, c) with $U(-\infty) = 0$ and $U(+\infty) = E_2$.

Since $\mathcal{R}_0^2 < 1$, two positive endemic equilibria, E_1 and E_2, exist. Equilibrium E_1 is unstable while E_2 is LAS. Thanks to the results obtained in Section 3, it is straightforward to check that assumption (L) holds and to conclude that a travelling wave solution connecting 0 and E_2 exists. See, for instance, Fig. 6.

In Fig. 7, we show that for u sufficiently small, the sign of the spreading speed can change. Thus, in the bistable case, for a given $a \gg 1$, there exist $u^\dagger$ and $u^{*,\dagger}$ such that for $u^\dagger < u < u^*$ the disease travelling wave moves forward, while for

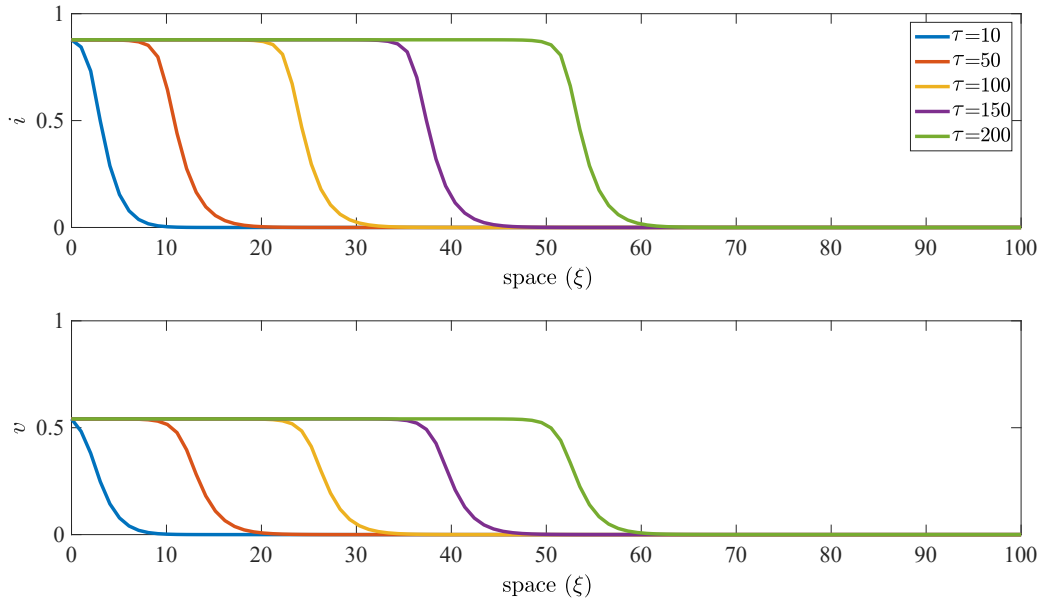

Figure 6: Bistable travelling wave solution of model (3) connecting the disease-free and endemic equilibria 0 and E_2 when $\mathcal{R}_0^2 = 0.96 < 1$. Here $u = 0.2$, other parameter values as in Fig. 1. The disease is invading, $c^* > 0$.

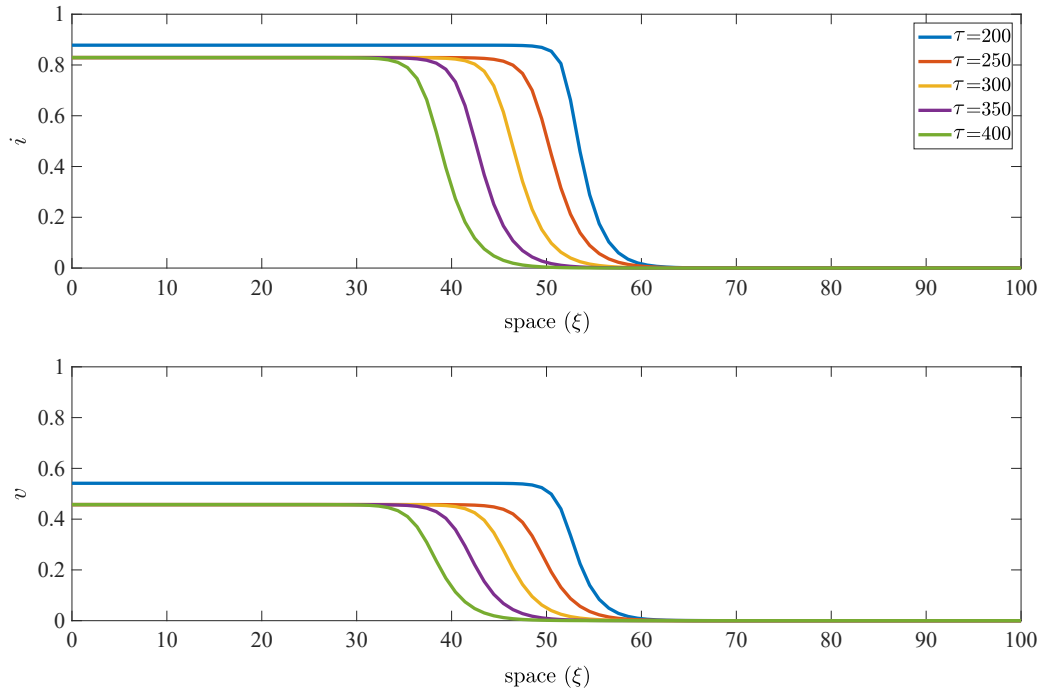

Figure 7: Bistable travelling wave solution of model (3) connecting the disease-free and endemic equilibria 0 and E_2 when $\mathcal{R}_0^2 = 0.72 < 1$. Here $u = 0.15$, other parameter values as in Fig. 1. Starting at $t = 200$ with the solution from Fig. 6 as initial condition, the spread is reversing, $c^* < 0$. This shows that a small variation of the parameter u (switching from $u = 0.2$ in Fig. 6 to $u = 0.15$ in this figure) can make the spreading speed switch from positive to negative. This is why the equilibrium prevalences decrease compared to initial conditions (at $t = 200$).

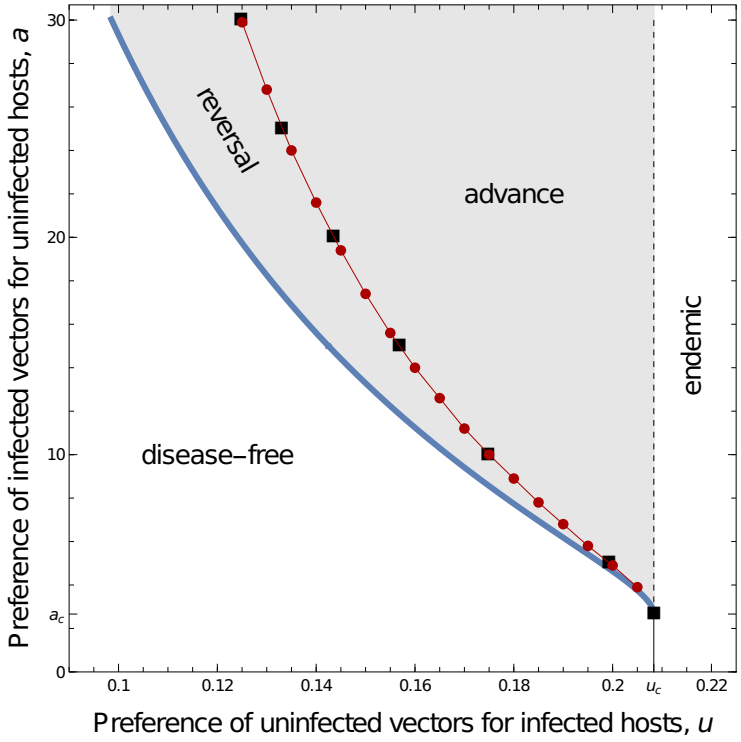

Figure 8: Within the bistable parameter domain (light grey), travelling waves connecting the disease-free and endemic equilibria can reverse or advance. The parameter domains of reversal and advance are separated by a curve corresponding to stalled waves with zero wave speed. Here, the zero-wave speed curve is obtained, on the one hand, by numerical integration of the PDE system (3) with $\rho = 1, \beta = 2.4, \theta = 2$ and identifying parameter values to result in zero wave speed, accurate to at least the third decimal place (grey squares). On the other hand, the zero wave speed curve was indicated by Eq. (25) in Appendix B.2 using a quasi-steady-state assumption (red points). Other curves as in Fig. 3.

$u^{*,\dagger} < u < u^{\dagger}$ the disease travelling wave moves backward. When $u < u^{*,\dagger}$ then the system converges to 0.

4.3.2 Quasi-steady-state approximation

For the case of a quasi-steady-state approximation (QSSA) (see Appendix B.2 for details), we can gain more information on the parameter domain for which the travelling wave moves forward or backward. The direction is given by the expression (25) in Appendix B.2.

Figure 8 marks the boundary between wave advancement and reversal by red dots. This boundary corresponds to stalled traveling waves with speed zero. The QSSA results match very well with the zero wave speeds in the original system without a quasi-steady-state approximation (dark grey squares). This match may be particularly surprising because we have chosen a time scale parameter of $\rho = 1$ for the simulations, while the QSSA is based on the assumption $\rho \gg 1$. However, Fig. 9

in Appendix B.2 suggests that the wave speed approximations do not deviate much from the exact solutions for small spreading speeds and $\rho \geq 1$. This behaviour might explain why the QSSA correctly locates the $c = 0$ curve in Fig. 8.

In the monostable case, the QSSA allows us to derive an explicit expression for the linear wave speed (see Eq. (23) in Appendix B.2), which is simply $c^* = 2\sqrt{\mathcal{R}_0^2 - 1}$. However, the linear spreading speed is only a lower bound of the actual spreading speed in somes cases (Fig. 11).

5 Discussion

We have shown that conditional vector preferences may result in bistability between the disease-free equilibrium and an endemic equilibrium. The novelty compared to Gandon (2018) and Cunniffe et al. (2021) is that bistability here occurs in the absence of any epidemiological feedback on vector population dynamics.

More specifically, we have shown that conditional vector preferences can cause a "backward bifurcation" (Fig. 2), meaning that $\mathcal{R}_0^2 < 1$ is not a sufficient condition for the disease to go extinct (e.g., Hadeler and van den Driessche, 1997).

5.1 Bistability conditions

We have shown that for bistability to occur, the following necessary conditions must be satisfied: $\mathcal{R}_0^2 < 1$, $a > 1$ and $u < u^* < 1$. The first condition ($\mathcal{R}_0^2 < 1$) means that the basic reproductive number of the pathogen is not large enough for the pathogen to invade a disease-free population. Hence, the disease-free equilibrium is locally stable. However, if the prevalence of the infection is initially high, and if infected vectors have a sufficiently strong preference for uninfected hosts ($a > 1$), we have shown that the pathogen may persist in the population (an endemic equilibrium is locally stable as well) even though $\mathcal{R}_0^2 < 1$. These two conditions ($a > 1$ and $\mathcal{R}_0^2 < 1$) are not too surprising. The third condition (implying $u < 1$) is less intuitive. To interpret it, we recall that $\mathcal{R}_0^2$ is proportional to u. If $\mathcal{R}_0^2 < 1$ in spite of $u > 1$ (uninfected vectors prefer infected hosts, which is advantageous for the pathogen), this means that the pathogen has poor reproductive abilities. Therefore, even if the prevalence of the infection is initially high, the pathogen still goes extinct. By

contrast, if $\mathcal{R}_0^2 < 1$ while $u < 1$ (uninfected vectors prefer uninfected hosts), it may be that the pathogen has strong enough reproductive abilities not to go extinct when its prevalence is initially high, and infected vectors prefer uninfected hosts ($\alpha > 1$).

5.2 Travelling waves

5.2.1 Monostable case

In the monostable case ($\mathcal{R}_0^2 > 1$), the disease invades the spatial domain. We have shown that the linear spreading speed depends only on ρ and $\beta\theta u$, meaning that it does not depend on α, the preference of infected vectors for uninfected hosts. The interpretation is the same as for the basic reproductive number, $\mathcal{R}_0^2 = \beta\theta u/\rho$, which does not depend on α either (Roosien et al., 2013; Gandon, 2018; Cunniffe et al., 2021). In a situation close to the disease-free equilibrium, like at the leading edge of the front, there are so few infected hosts that the preference of infected vectors for uninfected hosts has a negligible effect on the dynamics. However, even in the monostable case, the spreading speed may not be linearly determined (Fig. 5), implying that it may depend on α (Fig. 12). This is due to the fact that disease spread is not driven by the leading edge of the invasion front ("pulled wave"). Instead, the disease invasion is driven by the whole of the front ("pushed wave") (Stokes, 1976; Lewis and Kareiva, 1993). In particular, the disease spread may be maximum for intermediate prevalences because of the conditional preferences (similar to weak and strong Allee effects where population growth is strongest at intermediate densities). By contrast, dynamics of pulled waves are independent from the nonlinearities behind the leading edge of the front.

5.2.2 Bistable case

In the bistable case (requiring $\mathcal{R}_0^2 < 1$), the disease either invades or retreats, depending on parameter values. More specifically, travelling waves may have negative speeds, meaning that the disease retreats.

In an epidemiological context, such a "front reversal" has been shown to occur when host population dynamics in the absence of disease are bistable, due, for instance, to a strong Allee effect in the host (Hilker et al., 2005, 2007). However,

to our knowledge, such a phenomenon has seldom (Bocharov et al., 2016) been shown to occur when bistability is due solely to the epidemiological dynamics.

5.3 Biological implications

Although conditional vector preferences might occur in human and animal diseases, they have so far been shown mainly in plant diseases (Gandon, 2018). Therefore, we now discuss plant diseases more specifically.

Plant diseases are a main threat to global food security (Ristaino et al., 2021). Many plant diseases are caused by pathogens (viruses, bacteria and others) that are transmitted by insect vectors such as aphids, whiteflies, and others (Eigenbrode et al., 2018). Infected vectors can be attracted to uninfected plants. This is for instance the case for aphids, *Rhopalosiphum padi*, infected by the Barley yellow dwarf virus (BYDV) (Ingwell et al., 2012). In his review of evidence for conditional vector preferences, Gandon (2018) identified the volatile compounds emitted by infected plants as an attraction mechanism for (uninfected) vectors. For instance, plants infected by the *Cucumber mosaic virus* (CMV) or the *Tomato chlorosis virus* (ToCV) produce volatiles that attract aphids or whiteflies (Fereres et al., 2016). Note also that vectors can be attracted to infected plants by visual cues, such as, for instance, yellow leaves.

Since the basic reproductive number of the pathogen ($\mathcal{R}_0^2$) is proportional to u (the preference of uninfected vectors for infected hosts), a plant variety that emits fewer volatiles could be considered resistant to disease. When visual cues are responsible for vector preferences, a plant variety that expresses fewer symptoms, and is therefore less attractive to uninfected vectors, could also be considered resistant. Deployment of such resistant hosts might make it possible to obtain $\mathcal{R}_0^2 < 1$. We have shown that $u \geq 1$ (a preference of uninfected vectors for infected hosts) ensures disease extinction in this case ($\mathcal{R}_0^2 < 1$), since bistability requires $u < 1$. This means that breeding for varieties that emit, when infected, a concentration of volatiles that is lower than that of standard varieties is a possible strategy for the control of vector-borne diseases (in combination with other strategies such as roguing - i.e., removing - infected plants, for instance).

5.4 Mathematical prospects

An alternative for modelling vector preference could be density-dependent advection (in analogy to preytaxis, this could perhaps be called "hosttaxis"). It has been shown that preytaxis in the presence of disease, where predators are attracted to or repelled by infected prey, can speed up or even lead to irregularly fluctuating travelling waves (Bate and Hilker, 2019). While Chamchod and Britton (2011) considered a "hosttaxis" term in their model, it was only a vector bias towards infected hosts, regardless of whether the vector carries the pathogen or not. Modelling conditional vector preferences with a hosttaxis term is beyond the scope of this paper and is left for future research.

Acknowledgments: FMHa and YD gratefully acknowledge partial funding from the MODCOV19 CNRS platform. FMHa's visit in La Réunion (3P, Saint-Pierre) was partly supported by the European Agricultural Fund for Rural Development (EAFRD) within the DPP "Santé&Biodiversité" framework. YD is (partially) supported by the DST/NRF SARChI Chair in Mathematical Models and Methods in Biosciences and Bioengineering at the University of Pretoria, South Africa (Grant 82770). YD acknowledges the support of the Conseil Régional de la Réunion (France), the Conseil Départemental de la Réunion (France), the European Agricultural Fund for Rural Development (EAFRD) and the Centre de Coopération Internationale en Recherche Agronomique pour le Développement (CIRAD), France. The authors thank the reviewers for their insightful comments and helpful suggestions.

A Side results on the non-spatial model

A.1 Case $\mathcal{R}_0^2 = 1$ (boundary case)

If $\mathcal{R}_0^2 = 1$, or equivalently

$$u = \frac{\rho}{\beta\theta},$$

then $C = 0$ and $i^* = -B/A$. Using the above expression of u yields

$$i^* = 1 - \frac{1}{(\alpha-1)\left(\frac{\beta\theta}{(1+\theta)\rho} - 1\right)}.$$

If $\alpha = 1$, the endemic equilibrium does not exist. In what follows, we assume $\alpha \neq 1$.

Let the fraction of susceptible hosts at equilibrium be

$$s^* = \frac{1}{(\alpha-1)\left(\frac{\beta\theta}{(1+\theta)\rho} - 1\right)}.$$

We have:

$$s^* > 0 \Leftrightarrow \begin{cases} \frac{\beta\theta}{(1+\theta)\rho} > 1 & \text{if} \quad \alpha > 1\,, \\ \frac{\beta\theta}{(1+\theta)\rho} < 1 & \text{if} \quad \alpha < 1\,. \end{cases}$$

Assuming $s^* > 0$, $s^* < 1$ is equivalent to

$$(\alpha-1)\left(\frac{\beta\theta}{(1+\theta)\rho} - 1\right) > 1\,.$$

Two cases can then be distinguished:

- If $\alpha > 1$, $s^* < 1$ is equivalent to

$$\frac{\beta\theta}{(1+\theta)\rho} - 1 > \frac{1}{\alpha-1} \Leftrightarrow \frac{\beta\theta}{(1+\theta)\rho} > \frac{\alpha}{\alpha-1}\,.$$

- If $\alpha < 1$, $s^* < 1$ is equivalent to

$$\left(1 - \frac{\beta\theta}{(1+\theta)\rho}\right)(1-\alpha) > 1 \Leftrightarrow 1 - \frac{\beta\theta}{(1+\theta)\rho} > \frac{1}{1-\alpha} \Leftrightarrow -\frac{\beta\theta}{(1+\theta)\rho} > \frac{\alpha}{1-\alpha}\,,$$

  which is impossible.

Therefore, $0 < s^* < 1$ if and only if

$$\alpha > 1 \quad \text{and} \quad \frac{\beta\theta}{(1+\theta)\rho} > \frac{\alpha}{\alpha-1} > 1\,. \tag{16}$$

A.2 Case $\mathcal{R}_0^2 > 1$

To derive the expression of the endemic equilibrium, we consider three cases: $\alpha = 1$, $0 < \alpha < 1$ and $\alpha > 1$.

Case $a = 1$. If $a = 1$, then $A = 0$ and

$$i^* = -\frac{C}{B}.$$

Since $\mathcal{R}_0^2 > 1$,

$$B = -\left((1+\theta)u + \mathcal{R}_0^2 - 1\right) < 0\,.$$

Therefore,

$$i^* = \frac{\mathcal{R}_0^2 - 1}{(1+\theta)u + \mathcal{R}_0^2 - 1}\,.$$

We have $0 < i^* < 1$.

Case $0 \leq a < 1$. Since

$$B = -\left(\left((1+\theta)u + \mathcal{R}_0^2 - 1\right)a + (1-a)\right),$$

we deduce that $B < 0$. Then, we have three sub-cases to consider:

- If $u > u^*$, then $A < 0$. The relevant root is therefore the largest:

$$\frac{1}{2A}\left(-B - \sqrt{\Delta}\right),$$

  since the other root is negative.

- If $u = u^*$, $A = 0$. We obtain

$$i^* = \frac{\mathcal{R}_0^2 - 1}{\mathcal{R}_0^2 - 1 + \dfrac{1}{a}}\,. \tag{17}$$

  We have $0 < i^* < 1$.

- If $u < u^*$, then $A > 0$. The relevant root is therefore the smallest:

$$\frac{1}{2A}\left(-B - \sqrt{\Delta}\right),$$

  since both roots are positive.

Case $a > 1$. We again distinguish three sub-cases:

Table 1: The component i^* of the endemic equilibrium in the specific case $\mathcal{R}_0^2 > 1$, expressed as a function of A, B, C and $\Delta = B^2 - 4AC$.

	$0 < a < 1$	$a = 1$	$a > 1$
$u < u^*$	$\frac{1}{2A}\left(-B - \sqrt{\Delta}\right)$	$-\frac{C}{B}$	$\frac{1}{2A}\left(-B - \sqrt{\Delta}\right)$
$u = u^*$	$-\frac{C}{B}$	$-\frac{C}{B}$	$-\frac{C}{B}$
$u > u^*$	$\frac{1}{2A}\left(-B - \sqrt{\Delta}\right)$	$-\frac{C}{B}$	$\frac{1}{2A}\left(-B - \sqrt{\Delta}\right)$

- If $u > u^*$, then $A > 0$ and $B < 0$. The relevant root is therefore the smallest:

$$\frac{1}{2A}\left(-B - \sqrt{\Delta}\right),$$

since both roots are positive.

- If $u = u^*$, $A = 0$. We again find expression (17).

- If $u < u^*$, then $A < 0$. The relevant root is therefore the largest:

$$\frac{1}{2A}\left(-B - \sqrt{\Delta}\right),$$

since the other root is negative.

These results are summarized in Tab. 1.

A.3 Case $\mathcal{R}_0^2 < 1$

We here focus on the necessary condition $\Delta = B^2 - AC > 0$ for the existence of two endemic equilibria in the case $\mathcal{R}_0^2 < 1$. Using the notations $X = u(1+\theta) - 1$ and $Y = \mathcal{R}_0^2 - 1$ (Eq. (10)) yields the following expression of Δ as a quadratic function of a:

$$\Delta = (X-Y)^2 a^2 + 2(X(1+Y) + Y(1+X))a + 1\,.$$

Since $(X-Y)^2 > 0$, this parabola has a U-shape. We also have $\Delta(0) = 1 > 0$. Therefore, either there are two positive roots, a_c^- and a_c^+, or there are none. In the latter case, $\Delta > 0$ regardless of the value of a. In case there are two roots, the largest one,

$$a_c^+ = \frac{-((X(1+Y) + Y(1+X)) + 2\sqrt{XY(1+X)(1+Y)}}{(X-Y)^2},$$

can also be expressed as

$$a_c^+ = \left(\frac{\sqrt{-X(1+Y)} + \sqrt{-Y(1+X)}}{X-Y} \right)^2 .$$

Similarly, a_c^- can be expressed as

$$a_c^- = \left(\frac{\sqrt{-X(1+Y)} - \sqrt{-Y(1+X)}}{X-Y} \right)^2 .$$

Since $1+X = u(1+\theta) > 0$, $1+Y = \mathcal{R}_0^2 > 0$, and $Y = \mathcal{R}_0^2 - 1 < 0$, the existence of two conjugate roots requires $X = u(1+\theta) - 1 < 0$, or equivalently $u < u^*$.

We now focus on the condition $a > a_c^+$ (implying $\Delta > 0$) since it happens to coincide with the separatrix we numerically obtained in the parameter space (Fig. 3). Let us express a_c^+ as a function of the original parameters:

$$a_c^+ = \left(\frac{\sqrt{-(u(1+\theta)-1)\mathcal{R}_0^2} + \sqrt{-(\mathcal{R}_0^2-1)u(1+\theta)}}{u(1+\theta) - \mathcal{R}_0^2} \right)^2 , \tag{18}$$

or equivalently:

$$a_c^+(u) := \left(\frac{\sqrt{\left(1-\frac{u}{u^*}\right)\mathcal{R}_0^2} + \sqrt{(1-\mathcal{R}_0^2)\frac{u}{u^*}}}{\frac{\mathcal{R}_0^2}{u^*}(u_c - u^*)} \right)^2 .$$

Assuming $a_c^+(u)$ is defined for all $u \in [0, u_c]$ implies $u_c < u^*$.

In particular, since u_c is such that $\mathcal{R}_0^2 = 1$, we have

$$a_c^+(u_c) = \frac{1}{1-\frac{u_c}{u^*}} =: a_c . \tag{19}$$

The condition $a > a_c$ (implying $a > 1$) is equivalent to the condition we obtained for the existence of an endemic equilibrium in the boundary case $\mathcal{R}_0^2 = 1$, see Eq. (16). This means that in Fig. 3, the line $\mathcal{R}_0^2 = 1$ and the separatrix between the "disease-free" and "bistability" regions meet at the point (u_c, a_c).

B Side results on the spatial model

B.1 Existence of a minimum linear spreading speed

The function of the form $\xi \mapsto \exp(-\xi s)y$ is a solution of system (3) linearised around the disease-free equilibrium if and only if $scy = M_s y$, in which

$$M_s = \begin{pmatrix} -\rho & \beta \\ u\theta & -1+s^2 \end{pmatrix},$$

see Eq. (11). Since M_s is irreducible and, for all $s > 0$, essentially non-negative, the Perron-Frobenius theorem provides the existence of a unique eigenvalue κ_s of M_s associated to a positive eigenvector (Crooks, 1996)[Theorem 1.4]. Therefore, $sc = \kappa_s$. Since $c = \kappa_s/s$ is the dominant eigenvalue of $\frac{1}{s}M_s$, c is a convex function of s (Cohen, 1981).

B.2 Quasi-steady-state approximation

In this section, we make a quasi-steady-state approximation to reduce our model to a single dimension (similarly to Hamelin et al., 2016).

Model (3) can be equivalently expressed as:

$$\begin{aligned} \frac{1}{\rho} i_\tau &= \frac{\beta}{\rho} v \frac{a(1-i)}{a(1-i)+i} - i\,, \\ v_\tau &= \theta(1-v)\frac{ui}{ui+1-i} - v + v_{\xi\xi}\,. \end{aligned} \tag{20}$$

We consider the case where the infected vector removal rate $(m+l)$ is much lower than the removal rate of infected hosts r, so $\rho = r/(m+l) \gg 1$. This might happen in plant viruses if roguing occurs frequently relative to the vector lifespan ($r \gg m$), and the virus is persistent in the vector ($l = 0$).

We apply the quasi-steady-state approximation to the first equation of (20) to yield the fraction of infected hosts i directly in terms of the fraction of infected vectors v as

$$0 < i^{\#}(v) := \frac{\left(\frac{\beta}{\rho}v+1\right)a - \sqrt{\left(\left(\frac{\beta}{\rho}v-1\right)^2 a + 4\frac{\beta}{\rho}v\right)a}}{2(a-1)} < 1\,.$$

(It can be easily shown that the other root is greater than unity.)

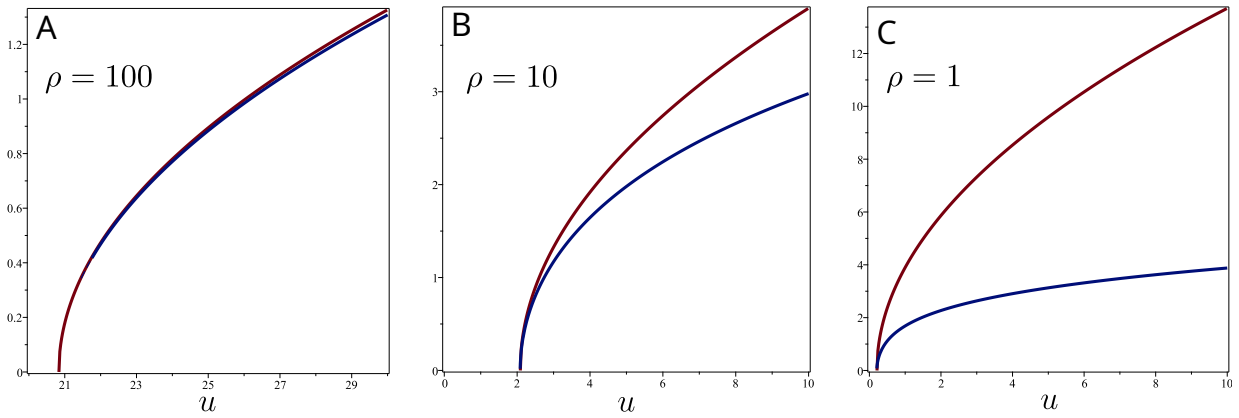

Figure 9: Exact linear spreading speed ($c^\star$, in red), as given by numerically solving Eq. (15), and approximated linear spreading speed (c^*, in blue), as given by Eq. (23) in the monostable case. Our quasi-steady-state-approximation (QSSA) assumes $\rho \gg 1$. It is therefore unsurprising that the QSSA performs badly when $\rho \leq 10$. However, the approximation does not seem to deviate much from the exact solution for small spreading speeds and $\rho \geq 1$. This might explain why the QSSA correctly locates the $c = 0$ curve in Fig. 8. Here, $\beta = 2.4\rho$, other parameter values as in Fig. 1.

This yields

$$v_t \approx \theta(1-v)\frac{u i^\sharp(v)}{u i^\sharp(v) + 1 - i^\sharp(v)} - v + v_{\xi\xi} =: W(v) + v_{\xi\xi}\,. \tag{21}$$

B.2.1 Monostable case ($\mathcal{R}_0^2 > 1$)

It is useful to notice that in the monostable case ($\mathcal{R}_0^2 > 1$), $W(0) = 0$, $W(v^*) = 0$, and $W(v) > 0$ for all $v \in (0, v^*)$. It is well known that if

$$\frac{W(v)}{v} < W'(0) \quad \text{for all} \quad v \in (0, v^*)\,, \tag{22}$$

the spreading speed of the wave is linearly determined (Stokes, 1976; Lewis and Kareiva, 1993):

$$c^* = 2\sqrt{W'(0)} = 2\sqrt{\frac{\beta}{\rho}\theta u - 1} = 2\sqrt{\mathcal{R}_0^2 - 1}\,. \tag{23}$$

Fig. 9 compares the linear speed under the QSSA (Eq. (21)) with the exact linear spreading speed given by Eq. (15). The QSSA performs well for large values of ρ, but performs increasingly badly for smaller values of ρ that do not meet the assumption $\rho \gg 1$ behind the QSSA.

Note, however, that if condition (22) is not satisfied, the spreading speed may

not be linearly determined. A sufficient condition for condition (22) not to hold is $W''(0) > 0$. We have

$$W''(0) = -\frac{2\frac{\beta}{\rho}u\theta\left((1+(u-1)a)\frac{\beta}{\rho}+a\right)}{a},$$

and so $W''(0) > 0$ is equivalent to

$$u < \frac{\frac{\beta}{\rho}(a-1)-a}{a\frac{\beta}{\rho}}.$$

Or equivalently,

$$(u-1)\frac{\beta}{\rho}+1<0 \quad \text{and} \quad a > \frac{\frac{\beta}{\rho}}{-((u-1)\frac{\beta}{\rho}+1)} =: \tilde{a}(u). \tag{24}$$

We also have

$$\tilde{a}(u_c) = \frac{\frac{\beta}{\rho}}{\frac{\beta}{\rho}-\frac{1}{\theta}-1} = \frac{1}{1-\frac{u_c}{u^*}} = a_c,$$

see Eq. (19). This means that the curve separating pulled waves (linear speed) with pushed waves (nonlinear speed) in the parameter plane "originates" at (u_c, a_c) (Fig. 10).

B.2.2 Bistable case ($\mathcal{R}_0^2 < 1$)

In the bistable case ($\mathcal{R}_0^2 < 1$), the wave speed is not linearly determined. However, it is well known (Fife and McLeod, 1977) that

$$\text{sign}(c^*) = \text{sign}\left(\int_0^{v_2^*} W(v)\mathrm{d}v\right), \tag{25}$$

where v_2^* is the stable nontrivial equilibrium of (21). Hence, the travelling wave has positive (negative) speed when the net area between the growth dynamics $W(v)$ of the approximated system (21) and the horizontal axis in the range between the disease-free state and the stable endemic state is positive (negative, respectively).

Figure 11 compares the linear spreading speed with the actual (numerically computed) spreading speed under the QSSA. It shows that in the bistable case ($u < u_c$), the spreading speed can be either negative or positive. In the monostable case

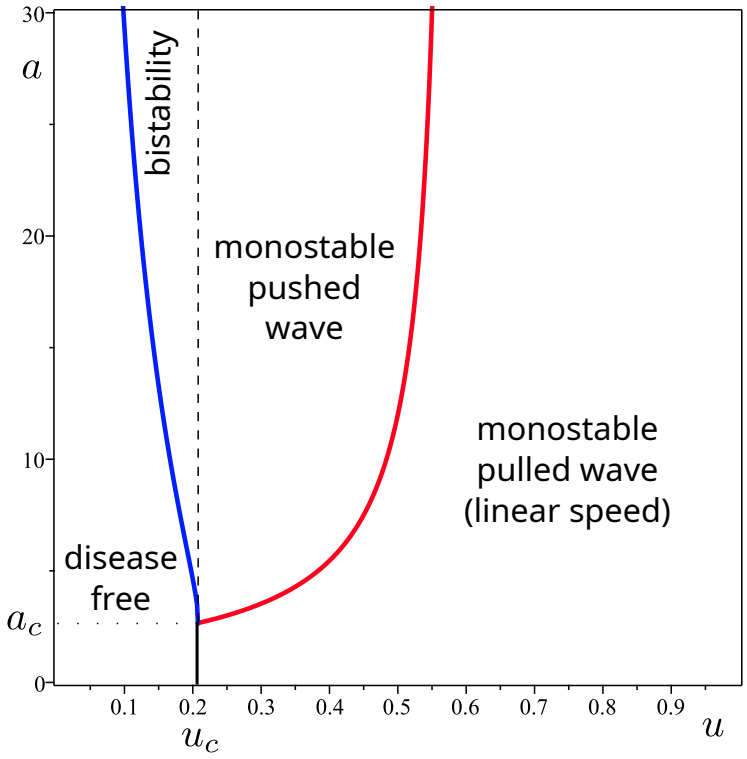

Figure 10: Two-parameter bifurcation analysis under the quasi-steady-state approximation (QSSA), i.e., model (21). The black line connecting $(u_c, 0)$ to (u_c, a_c) is the boundary between the monostable case with linear speed and the disease-free region. The blue line separates the disease-free region from the bistability region, as given by Eq. (18). The red line separates the monostable/pushed wave from the monostable/pulled wave (linear speed) region, as given by Eq. (24). Note that Eq. (24) only depends on β/ρ, while Eq. (18) only depends on θ and β/ρ through $\mathcal{R}_0^2 = \beta\theta u/\rho$. Parameter values: $\theta = 2$ and $\beta/\rho = 2.4$. Note, however, that ρ must be much greater than 1 for the QSSA to hold.

($u > u_c$), the actual spreading speed significantly deviates from the linear speed for u close to u_c, but the actual speed converges to the linear speed as u increases.

Figure 12 shows that the actual spreading does not depend on a when it is well approximated by the linear speed (for $u > 0.3$), while it increasingly depends on a as u decreases from $u = 0.3$. The dependency is greater in the bistable case ($u = 0.15$) than in the monostable pushed case ($u = 0.2$). As expected, the spreading speed is non-decreasing with a.

References

Anguelov, R., Dumont, Y., and Lubuma, J. (2012). Mathematical modeling of sterile insect technology for control of *Anopheles* mosquito. *Computers and Mathematics with Applications*, 64(3):374 – 389.

Bai, Z., Peng, R., and Zhao, X.-Q. (2018). A reaction–diffusion malaria model with seasonality and incubation period. *Journal of Mathematical Biology*, 77(1):201–

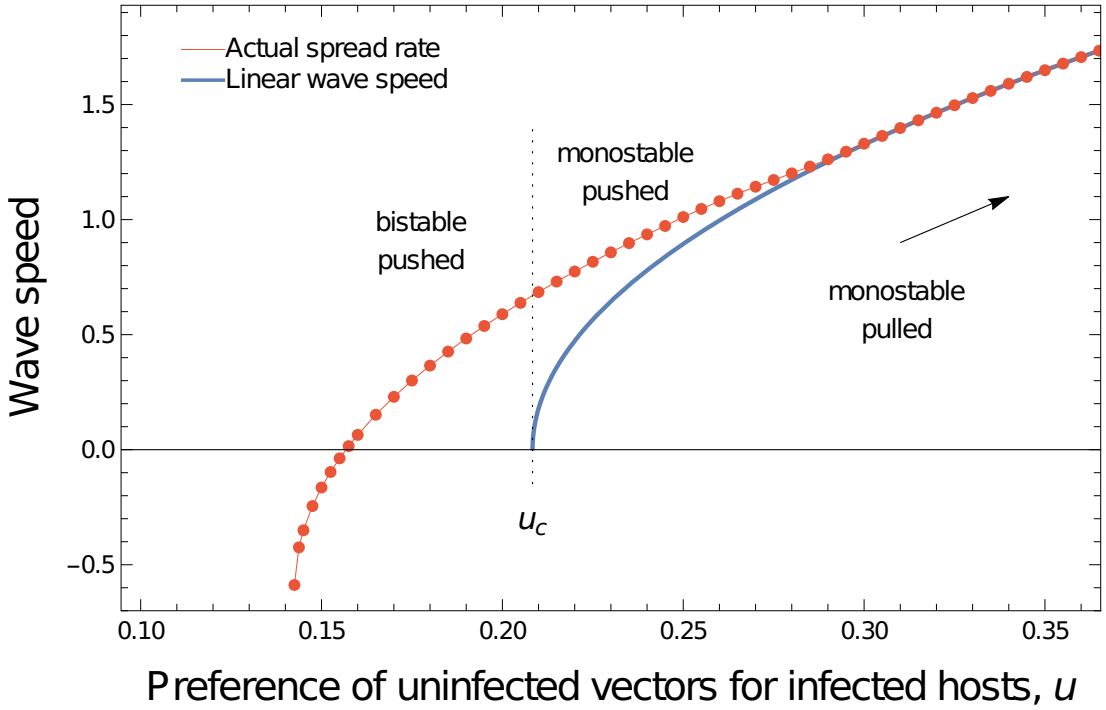

Figure 11: Comparing the linear wave speed, given by equation (23), with the actual (numerically computed) wave speed under the QSSA, i.e., model (21). Here, $\rho = 100$, $\beta = 2.4\rho$, other parameter values as in Fig. 1.

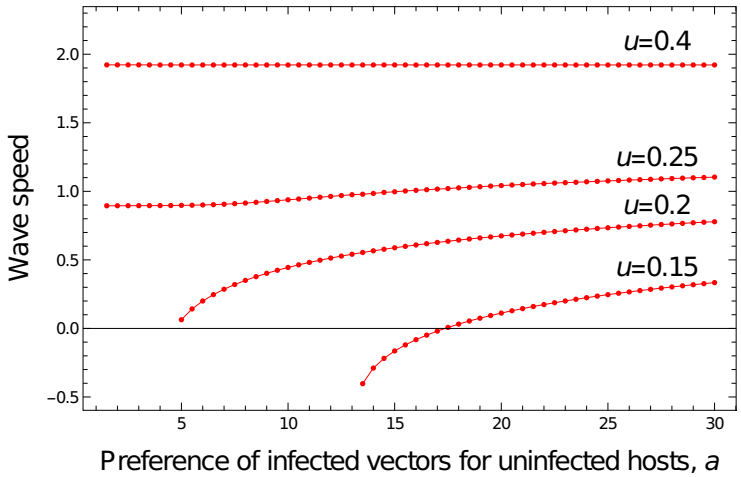

Figure 12: Shows whether and how the actual (numerically computed) spreading speed depends on a. This is for the QSSA, i.e., model (21), but the results are very similar in the original model (3), for $\rho = 1$. Here, $\rho = 100$, $\beta = 2.4\rho$, other parameter values as in Fig. 1.

228.

Bampfylde, C. J. and Lewis, M. A. (2007). Biological control through intraguild predation: case studies in pest control, invasive species and range expansion. *Bulletin of Mathematical Biology*, 69(3):1031–1066.

Bate, A. M. and Hilker, F. M. (2019). Preytaxis and travelling waves in an eco-epidemiological model. *Bulletin of Mathematical Biology*, 81(4):995–1030.

Blanc, S. and Michalakis, Y. (2016). Manipulation of hosts and vectors by plant viruses and impact of the environment. *Current Opinion in Insect Science*, 16:36–43.

Bocharov, G., Meyerhans, A., Bessonov, N., Trofimchuk, S., and Volpert, V. (2016). Spatiotemporal dynamics of virus infection spreading in tissues. *PLoS One*, 11(12):e0168576.

Buonomo, B. and Vargas-De-León, C. (2013). Stability and bifurcation analysis of a vector-bias model of malaria transmission. *Mathematical Biosciences*, 242(1):59–67.

Carr, J., Tungadi, T., Donnelly, R., Bravo-Cazar, A., Rhee, S., Watt, L., Mutuku, J., Wamonje, F., Murphy, A., Arinaitwe, W., Pate, A., Cunniffe, N., and Gilligan, C. (2020). Modelling and manipulation of aphid-mediated spread of non-persistently transmitted viruses. *Virus Research*, 277:197845.

Chamchod, F. and Britton, N. F. (2011). Analysis of a vector-bias model on malaria transmission. *Bulletin of Mathematical Biology*, 73(3):639–657.

Chapwanya, M. and Dumont, Y. (2018). On crop vector-borne diseases. Impact of virus lifespan and contact rate on the traveling-wave speed of infective fronts. *Ecological Complexity*, 34:119–133.

Cohen, J. E. (1981). Convexity of the dominant eigenvalue of an essentially non-negative matrix. *Proceedings of the American Mathematical Society*, 81:657–658.

Cornet, S., Nicot, A., Rivero, A., and Gandon, S. (2013). Malaria infection increases bird attractiveness to uninfected mosquitoes. *Ecology Letters*, 16(3):323–329.

Crooks, E. (1996). On the Vol'pert theory of travelling-wave solutions for parabolic systems. *Nonlinear Analysis: Theory, Methods & Applications*, 26(10):1621–1642.

Cunniffe, N. J., Taylor, N. P., Hamelin, F. M., and Jeger, M. J. (2021). Epidemiological and ecological consequences of virus manipulation of host and vector in plant virus transmission. *PLoS Computational Biology*, 17(12):e1009759.

Doli, V. (2017). *Phénomènes de propagation de champignons parasites de plantes par couplage de diffusion spatiale et de reproduction sexuée*. PhD thesis, Rennes 1.

Eigenbrode, S. D., Bosque-Pérez, N. A., and Davis, T. S. (2018). Insect-borne plant pathogens and their vectors: Ecology, evolution, and complex interactions. *Annual Review of Entomology*, 63:169–191.

Fagan, W. F., Lewis, M. A., Neubert, M. G., and van den Driessche, P. (2002). Invasion theory and biological control. *Ecology Letters*, 5:148–158.

Fang, J. and Zhao, X.-Q. (2009). Monotone wavefronts for partially degenerate reaction-diffusion systems. *Journal of Dynamics and Differential Equations*, 21(4):663–680.

Fang, J. and Zhao, X.-Q. (2014). Traveling waves for monotone semiflows with weak compactness. *SIAM Journal on Mathematical Analysis*, 46(6):3678–3704.

Fereres, A., Peñaflor, M. F. G. V., Favaro, C. F., Azevedo, K. E. X., Landi, C. H., Maluta, N. K. P., Bento, J. M. S., and Lopes, J. R. (2016). Tomato infection by whitefly-transmitted circulative and non-circulative viruses induce contrasting changes in plant volatiles and vector behaviour. *Viruses*, 8(8).

Fife, P. C. and McLeod, J. B. (1977). The approach of solutions of nonlinear diffusion equations to travelling front solutions. *Archive for Rational Mechanics and Analysis*, 65(4):335–361.

Gandon, S. (2018). Evolution and manipulation of vector host choice. *The American Naturalist*, 192(1):23–34.

Hadeler, K. and Lewis, M. (2002). Spatial dynamics of the diffusive logistic equation with a sedentary compartment. *Canadian Applied Mathematics Quarterly*, 10:473–499.

Hadeler, K. P. and van den Driessche, P. (1997). Backward bifurcation in epidemic control. *Mathematical Biosciences*, 146(1):15–35.

Hamelin, F. M., Castella, F., Doli, V., Marccais, B., Ravigné, V., and Lewis, M. A. (2016). Mate finding, sexual spore production, and the spread of fungal plant parasites. *Bulletin of Mathematical Biology*, 78(4):695–712.

Hamelin, F. M., Mammeri, Y .and Aigu, Y., Strelkov, S. E., and Lewis, M. A. (2022). Host diversification may split epidemic spread into two successive fronts advancing at different speeds. *Bulletin of Mathematical Biology*, 84(7):1–24.

Hilker, F. M., Langlais, M., Petrovskii, S. V., and Malchow, H. (2007). A diffusive SI model with Allee effect and application to FIV. *Mathematical Biosciences*, 206(1):61–80.

Hilker, F. M. and Lewis, M. A. (2010). Predator–prey systems in streams and rivers. *Theoretical Ecology*, 3:175–183.

Hilker, F. M., Lewis, M. A., Seno, H., Langlais, M., and Malchow, H. (2005). Pathogens can slow down or reverse invasion fronts of their hosts. *Biological Invasions*, 7(5):817–832.

Hosack, G. R., Rossignol, P. A., and Van Den Driessche, P. (2008). The control of vector-borne disease epidemics. *Journal of Theoretical Biology*, 255(1):16–25.

Ingwell, L. L., Eigenbrode, S. D., and Bosque-Pérez, N. A. (2012). Plant viruses alter insect behavior to enhance their spread. *Scientific Reports*, 2(1):1–6.

Janson, S. (2010). Resultant and discriminant of polynomials. Unpublished manuscript.

Kingsolver, J. G. (1987). Mosquito host choice and the epidemiology of malaria. *The American Naturalist*, 130(6):811–827.

Lacroix, R., Mukabana, W. R., Gouagna, L. C., and Koella, J. C. (2005). Malaria infection increases attractiveness of humans to mosquitoes. *PLoS Biology*, 3(9):e298.

Lewis, M., Renclawowicz, J., and den Driessche, P. v. (2006). Traveling waves and spread rates for a West Nile virus model. *Bulletin of Mathematical Biology*, 68(1):3–23.

Lewis, M. and Schmitz, G. (1996). Biological invasion of an organism with separate mobile and stationary states: Modeling and analysis. *Forma*, 11(1):1–25.

Lewis, M. A. and Kareiva, P. (1993). Allee dynamics and the spread of invading organisms. *Theoretical Population Biology*, 43(2):141–158.

Lewis, M. A. and van den Driessche, P. (1993). Waves of extinction from sterile insect release. *Mathematical Biosciences*, 116:221–247.

Li, B. (2012). Traveling wave solutions in partially degenerate cooperative reaction–diffusion systems. *Journal of Differential Equations*, 252(9):4842–4861.

Li, B., Weinberger, H. F., and Lewis, M. A. (2005). Spreading speeds as slowest wave speeds for cooperative systems. *Mathematical Biosciences*, 196(1):82–98.

Martcheva, M. (2015). *An Introduction to Mathematical Epidemiology*. Springer, New York.

Mauck, K. E., De Moraes, C. M., and Mescher, M. C. (2010). Deceptive chemical signals induced by a plant virus attract insect vectors to inferior hosts. *Proceedings of the National Academy of Sciences*, 107(8):3600–3605.

McElhany, P., Real, L. A., and Power, A. G. (1995). Vector preference and disease dynamics: a study of barley yellow dwarf virus. *Ecology*, 76(2):444–457.

Owen, M. R. and Lewis, M. A. (2001). How predation can slow, stop or reverse a prey invasion. *Bulletin of Mathematical Biology*, 63:655–684.

Rauch, J. and Smoller, J. (1978). Qualitative theory of the Fitzhugh-Nagumo equations. *Advances in Mathematics*, 27(1):12–44.

Ristaino, J. B., Anderson, P. K., Bebber, D. P., Brauman, K. A., Cunniffe, N. J., Fedoroff, N. V., Finegold, C., Garrett, K. A., Gilligan, C. A., Jones, C. M., et al. (2021). The persistent threat of emerging plant disease pandemics to global food security. *Proceedings of the National Academy of Sciences*, 118(23):e2022239118.

Roosien, B. K., Gomulkiewicz, R., Ingwell, L. L., Bosque-Pérez, N. A., Rajabaskar, D., and Eigenbrode, S. D. (2013). Conditional vector preference aids the spread of plant pathogens: results from a model. *Environmental Entomology*, 42(6):1299–1308.

Ross, R. (1911). Some quantitative studies in epidemiology. *Nature*, 87(2188):466–467.

Rothe, F. (1984). *Global solutions of reaction-diffusion systems*. Springer, Berlin.

Shoemaker, L. G., Hayhurst, E., Weiss-Lehman, C. P., Strauss, A. T., Porath-Krause, A., Borer, E. T., Seabloom, E. W., and Shaw, A. K. (2019). Pathogens manipulate the preference of vectors, slowing disease spread in a multi-host system. *Ecology Letters*, 22(7):1115–1125.

Sisterson, M. S. (2008). Effects of insect-vector preference for healthy or infected plants on pathogen spread: insights from a model. *Journal of Economic Entomology*, 101(1):1–8.

Smith, H. (2008). *Monotone dynamical systems: An introduction to the theory of competitive and cooperative systems*. American Mathematical Society, Providence, RI.

Stokes, A. (1976). On two types of moving front in quasilinear diffusion. *Mathematical Biosciences*, 31(3-4):307–315.

Wang, X. and Zhao, X.-Q. (2017). A periodic vector-bias malaria model with incubation period. *SIAM Journal on Applied Mathematics*, 77(1):181–201.

Wonham, M. J., de Camino-Beck, T., and Lewis, M. A. (2004). An epidemiological model for West Nile virus: invasion analysis and control applications. *Proceedings of the Royal Society of London. Series B: Biological Sciences*, 271(1538):501–507.

Xu, Z. and Zhang, Y. (2015). Traveling wave phenomena of a diffusive and vector-bias malaria model. *Communications on Pure & Applied Analysis*, 14(3):923.

Xu, Z. and Zhao, X.-Q. (2012). A vector-bias malaria model with incubation period and diffusion. *Discrete & Continuous Dynamical Systems-B*, 17(7):2615.